Nitrate reduction in streambed sediments: Effects of flow and biogeochemical kinetics

Chuanhui Gu,[1,2] George M. Hornberger,[1] Aaron L. Mills,[1] Janet S. Herman,[1] and Samuel A. Flewelling[1]

Received 9 March 2007; revised 25 July 2007; accepted 14 August 2007; published 28 December 2007.

[1] The effect of retention time on redox sequences along the hydrological flow path of groundwater discharging through low-relief coastal stream sediments and the subsequent impact on the fate of NO_3^- carried in the groundwater was examined in two intact cores. Rates of denitrification were determined for the organic-rich streambed sediments, and a macroscopic, multispecies, reactive transport model based on multiple Monod kinetics was developed to interpret and extend the experimental results. Regionalized sensitivity analysis and parameter estimation were used to determine a set of parameters that best describe the experimental data for one column. The calibrated model successfully replicated the spatial profiles of nitrate under both steady and transient conditions in the second column operated under different conditions. A dimensionless form of the model was used to examine how coupled biogeochemical reactions and hydrological transport processes operate within the stream sediments could be understood in terms of Peclet (ratio of advection to dispersion) and Damkohler numbers (the ratio of the characteristic time of transport to the characteristic time for reaction). At the study site, the Peclet number and the Damkohler numbers for both oxygen and nitrate are high ($Pe = 25$, $Da_N = 47.5$, and $Da_O = 40$). When $Pe > 5$, Damkohler numbers explain observed variations in nitrate removal rates; as the flow rate increases, the solute residence time in the reactive zone is shortened resulting in a lesser extent of reaction, such that more NO_3^- is delivered to the stream water.

Citation: Gu, C., G. M. Hornberger, A. L. Mills, J. S. Herman, and S. A. Flewelling (2007), Nitrate reduction in streambed sediments: Effects of flow and biogeochemical kinetics, *Water Resour. Res.*, *43*, W12413, doi:10.1029/2007WR006027.

1. Introduction

[2] Eutrophication of shallow marine and estuarine environments is a problem caused in part by the transport of dissolved nitrogen compounds from coastal groundwater to streams draining to the coastal bays and lagoons [*Denver et al.*, 2003; *Lowrance et al.*, 1997; *Phillips et al.*, 1993]. The planar surface of the streambed sediments is the interface between the surface water and the discharging groundwater. Biogeochemical reactions that occur near this groundwater–surface water interface (GSI) strongly affect the flux of nutrients to surface streams, especially acting to control fluxes of nitrogen from terrestrial to aquatic ecosystems [*Bencala et al.*, 1984; *Galavotti*, 2004; *Hedin et al.*, 1998; *Jones and Mulholland*, 2000; *Weiskel and Howes*, 1991]. High organic carbon contents in the sediments proximate to the GSI and permanently saturated conditions (i.e., low oxygen) favor nitrate (NO_3^-) attenuation by denitrification (the microbial conversion of NO_3^- to gaseous N_2) [*Burt et al.*, 1999].

[3] Denitrification is often concentrated in rather thin zones of sediment underlying the GSI [*Chen and Keeney*, 1974; *Sheibley et al.*, 2003a; *Whitmire and Hamilton*, 2005]. *Chen and Keeney* [1974] showed that 74–85% of nitrate pumped through intact cores extracted from lake sediments was lost to denitrification. Significant nitrate removal occurred in perfusion experiments on relatively short cores in a Minnesota stream [*Sheibley et al.*, 2003a]. *Whitmire and Hamilton* [2005] showed rapid nitrate removal in wetland sediments near the GSI.

[4] Given that sediments near the GSI are the most active sites for denitrification, it is not surprising that a common finding across field studies of NO_3^- removal processes in catchments is the importance of hydrology in influencing the extent of NO_3^- removal from groundwater [*Cirmo and McDonnell*, 1997; *Hill*, 1996]. The groundwater residence time influences the duration of denitrification acting to reduce the NO_3^- concentration of seepage water. The residence time can also indirectly affect NO_3^- attenuation by affecting oxygen and substrate supply in the near-GSI sediments. The impact of residence time on biochemical processes in groundwater is well known [*Brusseau et al.*, 1999a]. For example, the impact of residence time on biodegradation was examined in laboratory experiments reported by *Angley et al.* [1992], *Estrella et al.* [1993], and *Kelsey and Alexander* [1995]. They observed greater biodegradation at lower pore water velocities and for longer

[1]Department of Environmental Sciences, University of Virginia, Charlottesville, Virginia, USA.
[2]Now at Berkeley Water Center, University of California, Berkeley, California, USA.

0043-1397/07/2007WR006027$09.00

columns, which was attributed to the longer period of contact between the substrate and the microorganisms.

[5] In many locations, substantial denitrification removes NO_3^- as water passes through riparian buffer zones [*Haycock and Burt*, 1993; *Hedin et al.*, 1998; *Hill*, 1996]. On the other hand, denitrification may be relatively unimportant in some systems because of hydrogeological conditions [*Puckett and Hughes*, 2005]. The extent to which biogeochemical processes influence nitrate transport will depend on both the rates of fluid transport and chemical reactions [*Harvey and Fuller*, 1998]. A reasonable hypothesis is that rates of transport of nitrate to surface waters through the GSI are controlled by the rates at which microbial processes that catalyze denitrification proceed relative to the groundwater specific discharge and (often very short) path length of the biogeochemically active zone. Use of dimensionless ratios of hydrological and biogeochemical timescales [*Ocampo et al.*, 2006] is a powerful method for examining such hypotheses.

[6] A mathematical model that quantifies the kinetics of microbial processes under conditions of pore water flow through the GSI can be used to examine how different timescales can affect nitrate transport. Mathematical models for coupled advective-dispersive transport and oxidation-reduction have been used for groundwater systems [*Chen et al.*, 1992; *Kindred and Celia*, 1989; *Kinzelbach et al.*, 1991; *Molz et al.*, 1986; *Widdowson et al.*, 1988]. A single-component NO_3^- transport model with first-order reaction was applied in the study of NO_3^- attenuation at two agricultural catchments in Western Australia [*Ocampo et al.*, 2006]. The use of bulk reaction kinetics models is a useful phenomenonological approach to describe microbially mediated denitrification near the GSI [*Sheibley et al.*, 2003b]. None of these models, however, has included interactions of multiple redox species or Monod kinetics.

[7] We examined the hypothesis that the relationships among timescales for denitrification and for groundwater transport are useful for understanding the factors that determine nitrate fluxes to streams. Our work is based on observations at a field site near Oyster, Virginia. At this site, the change in NO_3^- concentration as the groundwater discharges into the stream is striking. The average NO_3^- concentration in 77 groundwater samples taken from several monitoring wells placed in the fields adjacent to and upgradient from the experimental hillslope was 8.95 ± 2.67 mg NO_3^--N L^{-1}. Typically values range from 5 to 20 mg NO_3^--N L^{-1}, depending on depth and location. On the other hand, stream concentrations averaged 2.0 mg NO_3^--N L^{-1} during the 4-year (a) field monitoring study. We conducted experiments on intact cores taken from this site to study biogeochemical processes of NO_3^- removal. A one-dimensional transport model using multiple Monod kinetics to simulate nitrate removal was developed and tested against the laboratory data. The model successfully described the transport and transformation of NO_3^- in redox transition zones. Results indicated that a Damkohler number, the ratio of a characteristic time of transport to a characteristic time for reaction, is of primary importance for determining the removal of the NO_3^- in water discharging through the GSI at our field site. We also used the model to explore how a Damkohler number and a Peclet number, the ratio of a characteristic time for advection to a characteristic time for dispersion, interact to control nitrate removal in general.

2. Methods

2.1. Intact Sediment Cores

[8] Our study site (37°15.5′N, 75°55.75′W) is in a low-relief watershed (4.8 km^2) drained by Cobb Mill Creek, on the property of the Anheuser-Busch Coastal Research Center (ABCRC) of the University of Virginia. The streambed of Cobb Mill Creek is mostly sand with variable amount of organic matter imbedded. The organic matter content in discrete sediment samples ranged between 0.05% and 20% by weight. The highest organic content occurs in a layer approximately 20 cm thick that is found at various locations in the upper 30 cm of the sediment. The average particulate organic matter (referred to as POC) content is about 3% for that 30-cm layer and is about 0.2% for the deeper sandy material. Two intact cores were obtained from the stream sediments of a 20-m-long reach of Cobb Mill Creek by driving sharpened 5-cm diameter PVC pipes vertically into the sediments. The pipes were driven below the water surface, capped with a rubber stopper, extracted, sealed at the bottom, and refrigerated in the lab within 4 h after collection. Each column was subsequently cut to obtain a relatively undisturbed section with a length of 45 or 50 cm, respectively.

[9] The columns were mounted vertically on a rack (Figure 1) for experiments conducted with varying flow rates to investigate the effect of retention time on NO_3^- removal. A detailed description of the laboratory column setup and the experiments is given by *Gu* [2007]. Briefly, artificial groundwater (AGW) was slowly pumped into the columns in an upflow direction and fully permeated the columns in between 1 and 2 d. The recipe for AGW used in the experiment was that used by *Bolster et al.* [1999] which was formulated based on the groundwater composition at this site; it contained (per liter of deionized water): 60 mg $MgSO_4{\cdot}7H_2O$, 20 mg KNO_3, 36 mg $NaHCO_3$, 36 mg $CaCl_2$, 35 mg $Ca(NO_3)_2$ and 25 mg $CaSO_4{\cdot}2H_2O$. Sampling ports were inserted along the length of the core after collection starting 5 cm from the column inlet with a vertical interval of 5 cm for the first 8 ports, 3 cm for the next three, and 2 cm for the last port.

[10] The columns were operated at room temperature (~24°C), upright, and under upflow conditions. A peristaltic pump was used to deliver the influent to the columns. Initially, the columns were flushed by NO_3^--free AGW to remove the background NO_3^- in the in situ pore water. The eluent solution then was switched to AGW with 15 mg L^{-1} NO_3^--N L^{-1}, the highest value of pore water nitrate concentration observed in stream piezometers [*Galavotti*, 2004]. Pore water samples were collected from intact sediment cores from each sampling port using a 3-mL syringe at 4-h intervals to determine the evolution of concentration profiles. Experiments were continued until an approximately steady state concentration of NO_3^--N (plateau of breakthrough curves) was obtained in the effluent (2 to 3 pore volumes).

[11] After the flow-through column experiment was finished, the sediment core was cut open lengthwise and immediately subsampled at 5-cm intervals using a detipped,

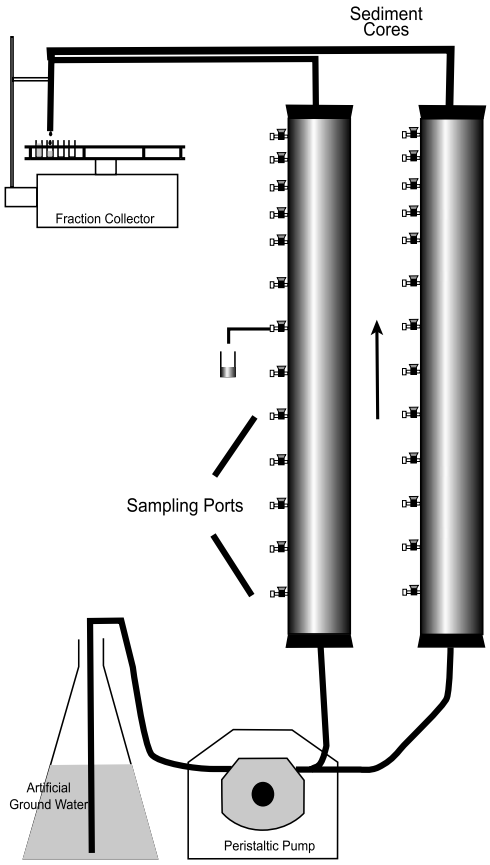

Figure 1. Schematic diagram of the laboratory column setup. A peristaltic pump was used to pump AGW into the intact cores from the bottom. Pore water samples were collected through the sampling ports. An automatic fraction collector was used for continuous sampling of effluent.

10-mL syringe as a minicorer. The subsamples were used to measure porosity, bulk density, and total organic matter content. Total organic matter in the sediment was determined by weight loss on ignition of the dried samples at 500°C for at least 24 h.

[12] Water samples were analyzed for nitrate and chloride on a Dionex® Ion Chromatograph using a Gilson® 234 Autoinjector and a Dionex IonPac AS4A® 4 × 250 mm analytical column. Prior to analysis by ion chromatography, water samples were centrifuged at approximately 6900 × *g* for 20 min to remove particles.

2.2. Model Development

2.2.1. Mathematical Formulation

[13] Because our field observations show that nitrate concentrations are relatively time invariant in both surface and groundwater, we assumed that the system is in steady state and that microbial biomass in the sediments is constant. The steady state obtained during column experiments should approximate the in situ situation because no organic substrate was added [*Battin et al.*, 2003; *Sheibley et al.*, 2003a]. Thus microbial growth was not included in the model. The active biomass was assumed to be attached to the sediment surfaces.

[14] In this study, we used a multiple-Monod equation [*Molz et al.*, 1986] to describe microbial reactions. The biological reactions simulated for the flow-through columns included aerobic respiration of dissolved organic matter followed by denitrification. The entire fraction of DOC, excluding any sorbed mass, was assumed to be labile and available. Noncompetitive inhibition was used to suppress denitrification while dissolved oxygen was present [*Widdowson et al.*, 1988].

[15] Different thicknesses of layers rich in POC exist in the intact cores from the field site. This solid organic matter cannot be used directly by microorganisms. Dissolution of the particles is a necessary step for energy acquisition. The POC-rich layers act as a source of labile DOC for the microbes. *Robertson and Cherry* [1995] presented data showing that the release of DOC from an actively denitrifying sediment layer amended with wood chips or sawdust is a kinetic process, indicating that the effluent DOC concentration is a function of water residence time in the layer. The DOC adsorption studies of *Jardine et al.* [1992] suggest that DOC release from POC by dissolution or desorption can be reasonably simulated by a first-order, mass transfer process.

[16] Four coupled equations, one for each dissolved species (O_2, NO_3^-, DOC) and one for the solid species (POC), compose the complete model (dimensional equations in Table 1). Nondimensional forms of the equations (nondimensional equations in Table 1) were used to examine how the rate-limiting processes operate outside the specific experimental results obtained with the columns [*Bahr and Rubin*, 1987; *Brusseau et al.*, 1999a, 1999b].

2.2.2. Numerical Solution

[17] The Galerkin finite element technique was selected for a numerical solution of the model equations. The dimensional equations (Table 1) can be generalized as

$$(L_x - L_\lambda)S = \frac{S^{n+1} - S^n}{\Delta t} \quad (1)$$

where S represents the mass concentration of the primary substrate, L_x is a transport operator, and L_λ represents the dual-Monod operator. A finite difference approximation replaces the time derivative, with n indicating the time level and $\Delta t = t^{n+1} - t^n$. Application of the weighted-residual finite element [*Hornberger and Wiberg*, 2005] results in a set of algebraic equations written as

$$([R] + [\lambda] + [Q])\{S\}^{n+1/2} = [Q]\{S\}^n + \{F\}^n \quad (2)$$

where [R] represents the tridiagonal coefficient matrices for the transport term, [λ] represents the multiple Monod decay matrices, [Q] is the element matrix for the time derivative term, and {F} is a specific flux vector introduced by boundary conditions.

[18] Equation (10) represents a system of nonlinear algebraic equations because the decay matrices [λ] at the current solution time depend on the unknown S at that time. These nonlinear equations were solved using the predictor-corrector method proposed by *Douglas and Jones* [1963]. The Douglas-Jones approximation uses two equations, a predictor and a corrector. Each equation advances the solution one half of a time increment. The predictor,

$$([R]^n + [\lambda]^n + 2[Q]^n)\{S\}^{n+1/2} = 2[Q]^n\{S\}^n + \{F\}^n \quad (3)$$

Table 1. Governing Equations of the Multispecies Reactive Transport Model

Dimensional Form[a]	Nondimensional Form[b]
$\frac{\partial O}{\partial t} = D\frac{\partial^2 O}{\partial x^2} - v\frac{\partial O}{\partial x} - V_O X \beta_O (\frac{C}{K_C+C})(\frac{O}{K_O+O})$	$\frac{\partial O^*}{\partial \tau} = \frac{1}{Pe}\frac{\partial^2 O^*}{\partial \xi^2} - \frac{\partial O^*}{\partial \xi} - Da_O X \beta_O \frac{1}{O_0} (\frac{O^*}{K_o^*+O^*})(\frac{C^*}{K_C^*+C^*})$
$\frac{\partial N}{\partial t} = D\frac{\partial^2 N}{\partial x^2} - v\frac{\partial N}{\partial x} - V_N X \beta_N \frac{K_I}{K_I+O}(\frac{C}{K_C+C})(\frac{N}{K_N+N})$	$\frac{\partial N^*}{\partial \tau} = \frac{1}{Pe}\frac{\partial^2 N^*}{\partial \xi^2} - \frac{\partial N^*}{\partial \xi} - Da_N X \beta_N \frac{K_I^*}{K_I^*+O^*}\frac{1}{N_0}\left(\frac{N^*}{K_N^*+N^*}\right)\left(\frac{C^*}{K_C^*+C^*}\right)$
$\frac{\partial C}{\partial t} = D\frac{\partial^2 C}{\partial x^2} - v\frac{\partial C}{\partial x} + \frac{\rho}{\varepsilon}\alpha(\overline{C} - K_d C) - V_O X_O \left(\frac{C}{K_C+C}\right)\left(\frac{O}{K_O+O}\right) - V_N X_N \frac{K_I}{K_I+O}\left(\frac{C}{K_C+C}\right)\left(\frac{N}{K_N+N}\right)$	$\frac{\partial C^*}{\partial \tau} = \frac{1}{Pe}\frac{\partial^2 C^*}{\partial \xi^2} - \frac{\partial C^*}{\partial \xi} + Da_C \frac{\rho}{\varepsilon}(K_{d0} - K_d C^*) - Da_N X_N \frac{K_I^*}{K_I^*+O^*}\frac{1}{N_0}\left(\frac{N^*}{K_N^*+N^*}\right)\left(\frac{C^*}{K_C^*+C^*}\right) - Da_O X_O \frac{1}{O_0}\left(\frac{O^*}{K_o^*+O^*}\right)\left(\frac{C^*}{K_C^*+C^*}\right)$
$\frac{d\overline{C}}{dt} = \alpha(K_d C - \overline{C})$	$\frac{dK_{d0}}{d\tau} = Da_C(K_d C^* - K_{d0})$

[a]Where ν is linear pore water velocity [LT^{-1}], D is the dispersion coefficient [L^2T^{-1}], O, N, C are the O_2, NO_3^- and DOC concentration, respectively, [ML^{-3}], V_O and V_N are the maximum specific uptake rates of the substrate for aerobic respiration and denitrification, respectively [T^{-1}], K_O, K_{N-} and K_C are the half-saturation constants for O_2, NO_3^- and DOC, respectively [ML^{-3}], X is the biomass concentration of facultative denitrifers [ML^{-3}], K_I is the inhibition constant for that substance [ML^{-3}], $\overline{C}$ is the particular organic carbon content [MM^{-1}], β is the uptake coefficient of the solutes for biodegradation process, K_d is the distribution coefficient [L^3M^{-1}], α is first-order mass transfer coefficient [T^{-1}], ρ is the bulk density [ML^{-3}], ε is the porosity (dimensionless).

[b]With the following dimensionless parameters: $\xi = x/L$; $\tau = tv/L$; $Pe = vL/D$; $O^* = O/O_0$; $N^* = N/N_0$; $C^* = C/C_0$; $Da_O = V_O L/v$; $Da_N = V_N L/v$; $Da_C = \alpha L/v$; $K_I^* = K_I/O_0$; $K_O^* = K_O/O_0$; $K_N^* = KN_I/N_0$; $K_C^* = K_C/C_0$. Where ξ is relative distance, τ is pore volume (dimensionless), L is the column length [L], Pe is Peclet number (dimensionless), O_0, N_0, and C_0 are the O_2, NO_3^-, and DOC boundary input concentration, respectively, [ML^{-3}], O*, N*, and C* are relative concentration of O_2, NO_3^-, and DOC, respectively (dimensionless). K_{d0} is initial distribution coefficient [L^3M^{-1}], Da_O, Da_N, Da_C are Damkohler numbers (dimensionless), K_O^*, K_N^*, and K_C^* are relative half saturation constants (dimensionless), K_I^* is relative inhibition constant (dimensionless).

is followed by the corrector

$$\left([R]^n + [\lambda]^{n+1/2} + [Q]^n\right)^{n+1} = [Q]^n\{S\}^n + \{F\}^{n+1/2} \quad (4)$$

The predictor-corrector approximation gives rise to systems of linear equations with a tridiagonal coefficient matrix that is easy to solve by the Gaussian elimination method. (The finite difference decoupling approach combined with the Thomas algorithm for solving system equations of PDE and ODE proposed by *Runkel and Chapra* [1993] provides an alternate for solving the equations and may have numerical advantages in some cases.)

[19] The model was verified through comparison with the analytical solution for steady state Monod kinetics with no dispersion and no decay [*Parlange et al.*, 1984] (Figure S1 showing the comparison in the auxiliary material)[1]. By properly adjusting time steps, we achieved oscillation-free results for all cases.

2.2.3. Initial and Boundary Conditions

[20] Particulate organic carbon contents were derived according to observed mean vertical profiles of POC [*Gu*, 2007]. Microbial biomass for facultative denitrifiers was set at each depth using data provided by J. M. Battistelli (unpublished data, 2005), which show a generally exponential decline with depth. The biomass profiles adapted in simulation were averaged values from measurements of 8 cores, which we take to be representative of our sediment cores. The total biomass was expressed as an aqueous concentration, mg L^{-1} of pore water, by using the bacterial number and a bacterial weight of 10^{-12} g per cell and measured porosity and bulk sediment density. Although the spatial distribution of biomass is critical to the model's success in reproducing the spatial profiles of constituents of interest, a precise estimate of biomass was not required because it is implicitly included as a lumped parameter in the model, i.e., it appears only as a product with uptake rates (Table 1).

[21] The boundary conditions chosen to represent the experimental conditions were a fixed concentration at the influent end of the column (Dirichlet type) and advective transport at the exit (Neumann type).

2.3. Parameter Estimation

[22] Prior values or ranges of values for the parameters in the model were obtained from the literature [*Chen et al.*, 1992; *Doussan et al.*, 1997; *MacQuarrie et al.*, 1990] or data collected from the site (e.g., POC content). An effective pore water velocity and dispersivity were found by fitting Cl^- breakthrough data to a 1-D nonreactive transport model CXTFIT 2.0 [*Toride et al.*, 1995]. The parameter values for this system have significant uncertainty, and many had to be estimated using the experimental results in an inverse procedure. Because there are eight parameters that require values, we chose to use a sequential approach to the inverse modeling to minimize the number of parameters to be estimated by a formal optimization procedure. Parameters were first eliminated that were approximated from experimental determinations (porosity, bulk density, etc.). For the rest of parameters, the regionalized sensitivity analysis (RSA) developed by *Hornberger and Spear* [1981] was employed to determine the relative importance of the

[1]Auxiliary materials are available in the HTML. doi:10.1029/2007WR006027.

parameters in the simulation model and results were used to select a subset of parameters for optimization.

[23] The RSA procedure involves Monte Carlo simulations, randomly sampling a set of parameter values from within designated ranges and running the transport model using the sampled set of values, as follows. We used Latin Hypercube Sampling [*McKay et al.*, 1979]. Each simulation run is then classified either as producing acceptable results (i.e., a simulated steady state NO_3^- concentration profile sufficiently "close" to observed values based on sum of squared errors (SSE)) or as not producing acceptable results. The cutoff value was chosen so that about 40% of the SSE values were smaller and 60% of the SEE values were larger than the cutoff value. This procedure is then repeated many times to give an accumulation of values of the parameters for which results are acceptable and another for which results are unacceptable. The subset of meaningful parameters that appear to account for the acceptability of the results is then identified. The distribution of the parameter values associated with acceptable results is compared with the distribution of parameter values associated with unacceptable results. If the two distributions are not different, the parameter is unimportant for simulating the designated acceptable behavior and is thus dropped for further calibration; if the two distributions differ by a large amount, the parameter is important and is selected for further calibration [*Hornberger et al.*, 1986].

[24] The microbial kinetic parameters and physical parameters were selected independently from uniform distributions over the physically meaningful range of the parameter [*Gu*, 2007]. If the parameter is one whose values can range over several orders of magnitude, the logarithm of the parameter was chosen from a uniform distribution [*Hornberger et al.*, 1985]. It was shown by preliminary model runs that convergence of statistical measures of model output was achieved if the number of model runs exceeds ten times the number of varied parameters. Thus 200 Monte Carlo simulations were run for the experiment. After accumulating the Monte Carlo runs into behavioral classes, the sensitivity of parameters can be judged by a comparison of the cumulative frequency distributions (CDF) of the accepted and rejected cases. A large value of $d_{m,n}$, the Kolmogorov-Smirnov two-sample statistic for the accepted and rejected cases, indicates a sensitive parameter [*Hornberger and Spear*, 1981]. The set of parameters to which results were deemed sensitive by the RSA were then fit to the observations from a single experimental column by minimizing the sum of squared errors between simulated and observed steady state profile of NO_3^-.

3. Results

3.1. Experimental Results

[25] The transient migration of a NO_3^- front was measured. A steady state NO_3^- profile developed after ~40 h (1.5 pore volume) of column operation (Figure 2). The rapid establishment of steady state conditions is due to the indigenous microbes in the intact cores that have adapted to the electron acceptors O_2 and NO_3^- existing in the groundwater at the field site. The NO_3^- concentration in the effluent was substantially lowered (20% of influent concentration) under steady state conditions. The cause of the loss was presumably due to microbially mediated denitrification, as no other nitrogenous material in the effluent was detected that could account for the NO_3^- that entered the column. A sharp oxidation-reduction gradient occurred within the top 15 cm of the sediment, the region that corresponded to the organic-matter-rich layer.

[26] When the flow rate through the column was increased, a higher nitrate concentration in the effluent was obtained, with the approach to the new equilibrium concentration occurring rapidly (Figure 3). When the flow was reduced back to the initial rate, NO_3^- in the effluent decreased correspondingly and settled at the previous steady state concentration.

3.2. Modeling Results

[27] Application of the RSA indicated that V_O and V_N (the maximum specific uptake rates of the substrate for aerobic respiration and denitrification, respectively) are the most important parameters for simulating observed behavior ($d_{m,n}$ = 0.57 and 0.59 for V_O and V_N, respectively, shown in Table 2). This is consistent with the expectation that not only denitrification but also aerobic respiration affects the fate of NO_3^-. The insensitivity of results to the two DOC-related parameters, α and K_d ($d_{m,n}$ = 0.12 and 0.14, respectively, shown in Table 2), indicates that the system is not limited by DOC. Sensitivity analysis (data not shown) showed that the NO_3^- reduction rate is not limited by DOC when POC content is at or above 2.1% [*Gu*, 2007].

[28] The values of all of the insensitive parameters were fixed at the median value of the ranges chosen as physically meaningful for the Monte Carlo simulations. The values for the two parameters identified in the RSA as important (V_O and V_N, the maximum uptake coefficient for aerobic respiration and denitrification, respectively) and for the important parameter for denitrification kinetics (the Monod half-saturation constant, K_N) were determined by optimization using data from one of the two experimental columns (column one, see Table 3, and Figure S3 showing the fit of the model results after calibration with experimental data is available in the auxiliary material).

[29] The calibrated model was tested against the experimental results from the other experimental column (column two). There is reasonable agreement between model predictions and the transient profile data (Figure 2). The rapid approach to steady state NO_3^- concentration profiles was successfully reproduced with the model (Figure 2 and Figure S2 showing simulated oxygen and DOC transient profiles in the auxiliary material), and the evolution of NO_3^- in the effluent with varying flow velocity is also replicated well by the model simulation (Figure 3).

3.3. Dimensional Analysis

[30] Moving beyond our experimental results to the more general case, there are four characteristic parameters, Da_O, Da_N, Pe, and Da_C (Table 1), that control biodegradation during transport. Da_O, Da_N, and Da_C are defined as Damkohler numbers of aerobic respiration, denitrification, and POC dissolution, respectively. A Damkohler number is a dimensionless number relating the timescale for reaction to the timescale for advection. The Peclet number, Pe, is a dimensionless number relating a timescale for advection to a timescale for dispersion. When organic carbon is not limiting, Da_O, Da_N and Pe are three factors determining

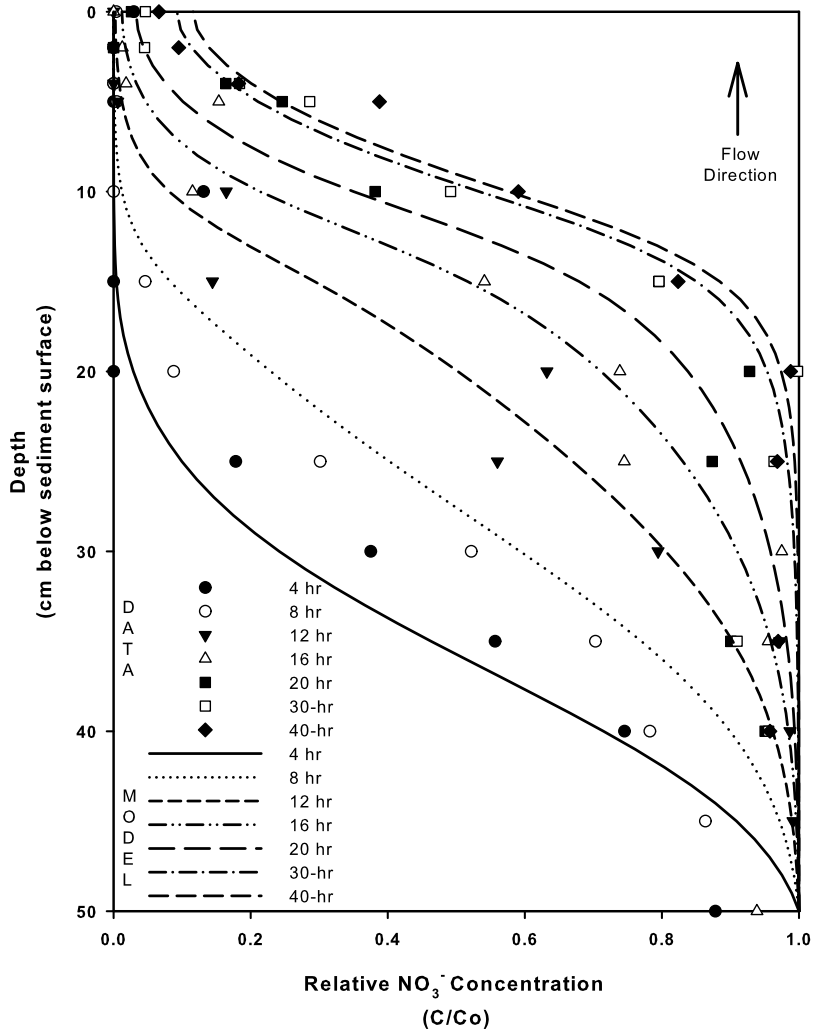

Figure 2. NO_3^- transient profiles of column two during the step input for simulation with 1.1 and percnt; POC content at v = 2 cm h^{-1}. Initial NO_3^- concentrations were zero through the column. Flow direction is upward.

NO_3^- transport. Given the fact Da_O correlates tightly to Da_N in most case (i.e., both aerobic respiration and denitrification are conducted by the facultative denitrifier), we chose to address the effect of Da_N and Pe on NO_3^- removal. We also examined the effect of influent NO_3^- concentration on nitrate removal as this value appears in the dimensionless equations because of the nonlinearity of the Monod kinetic term.

[31] Da_N and Pe jointly affect the magnitude of nitrate removal during transport (Figure 4a). The fraction of NO_3^- removed increases as the magnitude of Da_N increases. No measurable nitrate loss occurred at low Da_N (<1), because biodegradation is constrained by either the very short residence time (i.e., rapid flow) or very low reaction rate (i.e., lack of biomass). In the case of fixed Da_N,the fraction of nitrate removed also increases as the magnitude of Pe increases and reaches a plateau when Pe > 10, so increasing flow velocity at high flow rates will decrease NO_3^- loss by decreasing the Damkohler number only and not by changing the Peclet number. Maximum removal is achieved at high values of both Pe (>10) and Da_N (>20).

[32] Insignificant NO_3^- loss occurred at very low Pe (<1) due to diffusion-limited biodegradation. In this low-Pe region, increasing pore water velocity will increase Pe, representing an increase in the supply of carbon substrate to the microorganisms. Consequently, the NO_3^- removal increases. Increases in velocity, however, not only increase Pe but also decrease Da_N. These effects act in the opposite directions to influence NO_3^- removal. Nitrate loss therefore will depend on the balance between the hydrological and biogeochemical factors.

[33] The nonlinearity of Monod kinetics of denitrification leads to the appearance of the influent nitrate concentration (N_0) in the dimensionless equations (second nondimensional equation in Table 1). The fraction of removal of NO_3^- decreases when NO_3^- concentration in influent increases (Figure 4b).

4. Discussion

[34] Groundwater–surface water interfaces are biogeochemically active zones in which hydrological transport can

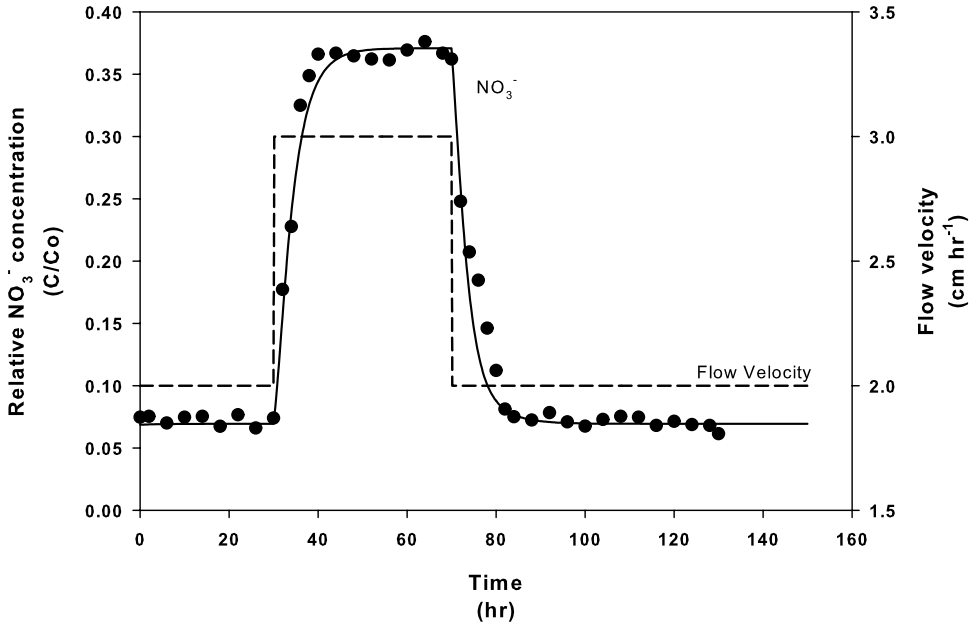

Figure 3. Measured and simulated effluent nitrate breakthrough in response to applied stepwise increased flow rates for column two.

influence nutrient loading from groundwater discharging to surface water [*Duff and Triska*, 2000; *Sheibley et al.*, 2003a]. The region of highest reactivity is often a narrow one adjacent to the stream channel. This situation indicates that experiments with intact sediment cores can be used to study in situ conditions as long as natural chemical gradients and biomass distributions are mimicked and the flows that influence biogeochemical processes are accurately simulated. At Cobb Mill Creek, a sediment core of around 50 cm in length is sufficient to study NO_3^- reduction under natural groundwater discharge conditions of upward flowing groundwater moving vertically through the streambed sediments with little hyporheic mixing. When NO_3^- was pumped through such columns, a high denitrification capacity was observed in the last 20 cm of the flow path, and a chemical profile similar to the in situ pore water profiles found in the field site developed [*Galavotti*, 2004]. The rapid removal of NO_3^- indicates excess carbon availability in the sediment. These findings are similar to those in perfusion core experiments by *Sheibley et al.* [2003a].

[35] Our results showing that effluent nitrate concentrations increase with increasing flow rates have implications for delivery of nitrate to coastal streams. Seasonal discharge variability and transient hydrological events will change groundwater flow velocity and, thus associated NO_3^- loading significantly. For example, if groundwater velocity were to increase in storm events, high concentration of NO_3^- could be released to the surface water because of the lower residence time in sediments near the GSI.

[36] Although we assumed the DOC concentration to be limited by the amount of POC and the rate of conversion to dissolved form, our results show that in Cobb Mill Creek sediments, DOC is not limiting. Approximately steady state conditions have been maintained for several months in flow-through columns, indicating that there is a large organic carbon pool in the sediments that is not easily depleted by microbial degradation. The carbon release Damkohler number, Da_C, is relatively high for our site. Thus, as long as POC is available, carbon is not limited by the processes of dissolution and desorption. A characteristic time for depletion of DOC is embodied in the coefficient α (fourth dimensional equation in Table 1). The maximum rate of depletion is $e^{-\alpha t}$. For a 1-month period, $e^{-\alpha t}$ is about 0.7, so only 30% of the material would be lost. In this area of Virginia, it is safe to assume that hydrological events would bury new POC in the streambed sediments on a timescale that would replenish POC prior to significant depletion. The simple assumption of excess DOC supply [*Ocampo et al.*, 2006] is met in the streambed sediments underlying the GSI where denitrification is active at our site.

[37] The parameter values of the transport model for simulating the transient state and steady state utilization of multiple electron acceptors (O_2 and NO_3^-) during groundwater seepage for our sediments is consistent with published results. Half-saturation constants of nitrate (K_N) in studies

Table 2. Results of the Kolmogorov-Smirnoff Test for the Transport Model

Parameter	Symbol	$d_{m,n}$[a]
Maximum uptake coefficient of aerobic respiration	V_O	0.57
Maximum uptake coefficient of denitrification	V_N	0.59
Inhibition constant of O_2	K_I	0.17
Monod half-saturation constant for O_2	K_O	0.17
Monod half-saturation constant for NO_3^-	K_N	0.10
Monod half-saturation constant for substrate	K_C	0.12
Mass transfer coefficient	α	0.12
Distribution coefficient	K_d	0.14

[a]Value of maximum distance in the Kolmogorov-Smirnov test.

Table 3. Input Parameters for the Laboratory Simulation of Column One

Parameter	O_2/NO_3^-
Maximum specific growth rate, V_O and V_N, h^{-1}	1.9[a]/1.6[a]
Half-saturation constant of electron acceptors, K_O and K_N, mg L^{-1}	0.2/2[a]
Half-saturation constant of electron donor, K_C, mg L^{-1}	1/1
Uptake coefficient, β	2/2
Mass transfer coefficient of POC, α, h^{-1}	5×10^{-5}
Distribution coefficient of DOC, K_d, L kg^{-1}	50
Inhibition constant, K_I, mg L^{-1}	0.01
Longitudinal grid spacing, cm	1
Column length, L, m	0.5
Effective porosity, ε	0.28
Longitudinal dispersion coefficient, D, cm^2 h^{-1}	4
Linear velocity, ν, cm h^{-1}	2.0
Simulation time, h	340
Time step size, h	0.2
O_2 for x = 0, O_0, mg L^{-1}	8
NO_3^- for x = 0, N_0, mg L^{-1}	15
DOC for x = 0, C_0, mg L^{-1}	0

[a]Calibrated with experimental results.

of denitrification in soil and sediment range from 0.21 to 4.06 mg N L^{-1}, with most values reported between 1 and 4 mg N L^{-1} [*Esteves et al.*, 1986; *Murray et al.*, 1989; *Oremland et al.*, 1984]. The half-saturation constant of NO_3^- in the calibrated model was 2 mg N L^{-1}, a value comparable to many of the published values, for example 3.06 mg N L^{-1} [*Messer and Brezonik*, 1984], 2.1 mg N L^{-1} [*Schipper et al.*, 1993], and 1.25 mg N L^{-1} [*Maag et al.*, 1997]. Our study shows a mean apparent maximum denitrification rate V_a value of 1.1 mg N L^{-1} h^{-1}(defined as = V_N*X (first and second dimensional equations in Table 1)), comparable to the value of 1.51 mg N L^{-1} h^{-1} found in the upper horizon in a wet meadow soil [*Maag et al.*, 1997], 0.46 mg N L^{-1} h^{-1} in riparian soils [*Schipper et al.*, 1993], 1.8 mg N L^{-1} h^{-1} in agricultural soils and a pond sediment [*Murray et al.*, 1989],and 1.26 mg N L^{-1} h^{-1} measured in a lake sediment at 35.5°C [*Messer and Brezonik*, 1984]. *Sheibley et al.* [2003b] observed a mean first-order rate coefficient for denitrification of 1.5 h^{-1}, which would imply a V_a of 3 mg N L^{-1} h^{-1} assuming a half-saturation constant of 2 mg N L^{-1}. Our V_a value, however, is several orders of magnitude higher than those V_a values converted from first-order rate coefficients for denitrification reported in several studies from soil systems [*Starr et al.*, 1974]. The relatively high reaction rates in this study may typify streambed (or other wet) environments with continually renewed substrates and nitrate.

[38] The dependence of NO_3^- reduction on flow rate demonstrates that the redox reaction is kinetically controlled; or, in other words, the timescale for NO_3^- reduction is on the order of the timescale for advective transport. The NO_3^- removal decreases as the ratio of reaction to transport rates decreases. This is because as the flow rate increases, the solute residence time in the reactive zone is shortened resulting in lesser extent of reaction. Furthermore, oxygen must be depleted before denitrification can become effective and the oxygen consumption reaction zone changes with flow rate: an increase in pore water velocity decreases the thickness of the anaerobic zone because the oxygen front propagates farther into the column. Consequently, the zone in which denitrification can occur shrinks, resulting in higher effluent nitrate concentrations.

[39] For our site, the Peclet number and the Damkohler numbers for both oxygen and nitrate are high (Pe = 25, Da_N = 47.5, and Da_O = 40). Thus we are in a region where changes in Da_N will dominate the response in terms of net nitrate removal (Figure 4a). The results of our dimensional analysis show that this will be the case whenever the Peclet number is sufficiently high. In these cases, the proposal of *Ocampo et al.* [2006] that a Damkohler number can explain observed variation in nitrate removal rates will hold. In cases where Pe falls below about 5, however, changes in

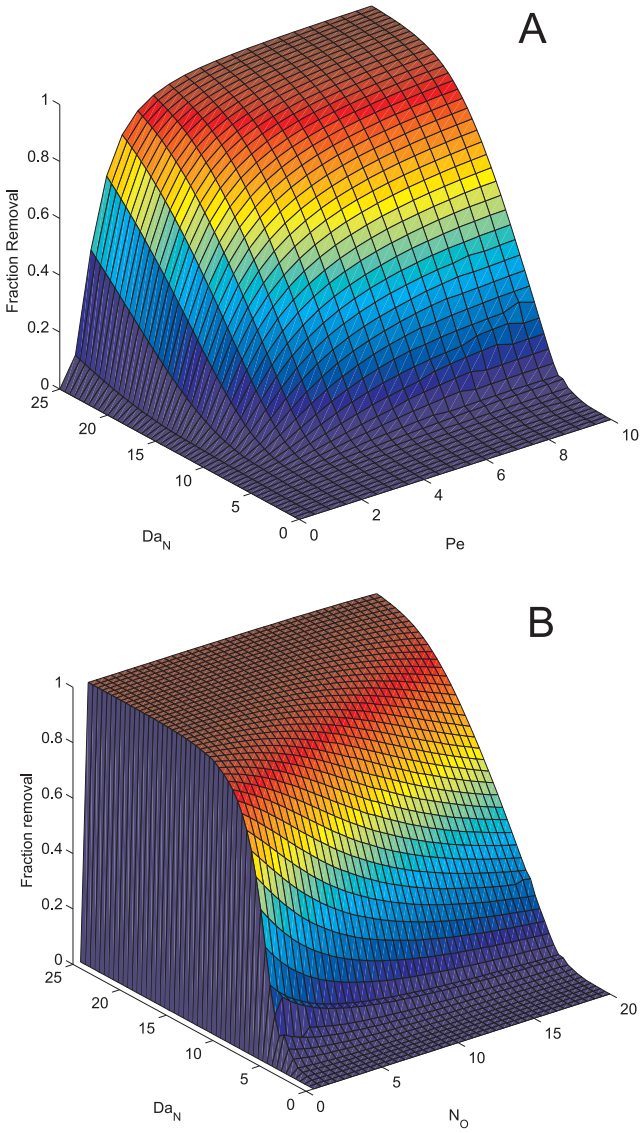

Figure 4. (a) Response surface of fraction of NO_3^- removal to Da_N number and Peclet number and (b) response surface of fraction removal to Da_N and the influent NO_3^- concentration (N_{in}). All the other parameters are held constant as those in baseline simulation.

both the Pe and the Da as a result of variations in flow rates will exert control on net nitrate removal.

[40] For our site, the influent concentration of NO_3^- is about 15 mg L^{-3}, corresponding to the region where the fraction of NO_3^- removal is influenced by the change of influent concentration of NO_3^- (Figure 4b). Only when NO_3^- concentration is much lower than the half-saturation constant K_N, i.e., $\ll$2 mg L^{-3} NO_3^--N in the present case, is the fraction of NO_3^- removal independent of influent concentration of NO_3^-. In most cases, however, NO_3^- concentration is high (>EPA drinking water standard which is 10 mg L^{-1} NO_3^--N) in polluted aquifers. Under such conditions it is essential to include the nonlinear effect of influent concentration on Monod reaction kinetics in the transport model in order to evaluate the NO_3^- removal.

[41] Our results indicated that most of the NO_3^- (>80%) that is being transported through streambed sediment at the hillslope site at Cobb Mill Creek is removed by uptake in sediments near the GSI. Two conditions are generally necessary for streambed sediment removal to be significant. First, timescales of the chemical reaction and pore water transport in the streambed must be similar, and second, the water flow must be fast enough to avoid diffusion-limited conditions. If these conditions are met for a major portion of the stream length, streambed sediment removal of nitrate is likely be effective at the catchment scale.

[42] *Ocampo et al.* [2006] proposed using a Damkohler number based on a first-order reaction for nitrate removal to explain how hydrological and biogeochemical processes occurring within a riparian zone interact to effect net nitrate removal. We have presented a generalization of this approach to include potential effects of multiple electron acceptors and the relative importance of dispersion to advection. In principle, the various dimensionless groups in our formulation are related to several measurable physical and biogeochemical factors. The microbial reaction rate constant is mainly determined by organic matter content supplied by stream riparian vegetation and seepage velocity depends on physical properties of the sediment and the hydraulic gradient, which is determined by landscape topography. The nutrient buffer capacity of riparian zones will depend on the complex combination of all these landscape and hydrogeomorphologic variables. Further work is required to determine if the generalized framework proposed here can lead to a deeper understanding of how the various factors interact to affect net nitrate removal [*Ocampo et al.*, 2006; *Vidon and Hill*, 2004]. A combination of a Peclet number and Damkohler numbers may provide an index to define wide variations in the efficiency of riparian zones as a nutrient buffer, such as the tenfold differences in NO_3^- export from adjacent catchments observed in the Canadian Shield [*Schiff et al.*, 2002] and observation of high nutrient buffer capacities of riparian zones [*Hedin et al.*, 1998; *Hill et al.*, 2000] in some areas versus the poor nutrient buffer effect of riparian zones found elsewhere [*Puckett and Hughes*, 2005].

[43] **Acknowledgments.** This research was supported by funding from the National Science Foundation under NSF-EAR 0208386. We thank Holly S. Galavotti and Joseph M. Battistelli for assistance with lab and field work. The Virginia Coast Reserve LTER provided accommodation and logistical support during the field work.

References

Angley, J. T., M. L. Brusseau, W. L. Miller, and J. J. Delfino (1992), Nonequilibrium sorption and aerobic biodegradation of dissolved alkylbenzenes during transport in aquifer material—Column experiments and evaluation of a coupled-process model, *Environ. Sci. Technol.*, *26*(7), 1404–1410.

Bahr, J. M., and J. Rubin (1987), Direct comparison of kinetic and local equilibrium formulations for solute transport affected by surface-reactions, *Water Resour. Res.*, *23*(3), 438–452.

Battin, T. J., L. A. Kaplan, J. D. Newbold, and S. P. Hendricks (2003), A mixing model analysis of stream solute dynamics and the contribution of a hyporheic zone to ecosystem function, *Freshwater Biol.*, *48*(6), 995–1014.

Bencala, K. E., V. C. Kennedy, G. W. Zellweger, A. P. Jackman, and R. J. Avanzino (1984), Interactions of solutes and streambed sediment: 1. An experimental-analysis of cation and anion transport in a mountain stream, *Water Resour. Res.*, *20*(12), 1797–1803.

Bolster, C. H., A. L. Mills, G. M. Hornberger, and J. S. Herman (1999), Spatial distribution of deposited bacteria following miscible displacement experiments in intact cores, *Water Resour. Res.*, *35*(6), 1797–1807.

Brusseau, M. L., M. Q. Hu, M. J.-Wang, and R. M. Maier (1999a), Biodegradation during contaminant transport in porous media. 2. The influence of physicochemical factors, *Environ. Sci. Technol.*, *33*(1), 96–103.

Brusseau, M. L., L. H. Xie, and L. Li (1999b), Biodegradation during contaminant transport in porous media: 1. Mathematical analysis of controlling factors, *J. Contam. Hydrol.*, *37*(3–4), 269–293.

Burt, T. P., L. S. Matchett, K. W. T. Goulding, C. P. Webster, and N. E. Haycock (1999), Denitrification in riparian buffer zones: The role of floodplain hydrology, *Hydrol. Processes*, *13*(10), 1451–1463.

Chen, R. L., and D. R. Keeney (1974), The fate of nitrate in lake sediment columns, *Water Resour. Bull.*, *10*(6), 1162–1172.

Chen, Y., L. M. Abriola, P. J. J. Alvarez, P. J. Anid, and T. M. Vogel (1992), Modeling transport and biodegradation of benzene and toluene in sandy aquifer material: comparisons with experimental measurements, *Water Resour. Res.*, *28*(7), 1833–1847.

Cirmo, C. P., and J. J. McDonnell (1997), Linking the hydrologic and biogeochemical controls of nitrogen transport in the near-stream zones of temperate-forested catchments: A review, *J. Hydrol.*, *199*(1–2), 88–120.

Denver, J. M., S. W. Ator, L. M. Debrewer, M. J. Ferrari, J. R. Barbaro, T. C. Hancock, M. J. Brayton, and M. R. Nardi (2003), Water quality in the Delmarva Peninsula: Delaware, Maryland, and Virginia, 1999–2001, *U.S. Geol. Surv.*, *1228*.

Douglas, J., and B. F. Jones (1963), On predictor-corrector methods for nonlinear parabolic differential equations, *J. Soc. Ind. Appl. Math.*, *11*(1), 195–204.

Doussan, C., G. Poitevin, E. Ledoux, and M. Detay (1997), River bank filtration: Modelling of the changes in water chemistry with emphasis on nitrogen species, *J. Contam. Hydrol.*, *25*(1–2), 129–156.

Duff, J. H., and F. J. Triska (2000), Nitrogen biogeochemistry and surface-subsurface exchange in streams, in *Streams and Ground Waters*, edited by J. B. Jones and P. J. Mulholland, pp. 197–220, Academic, London.

Esteves, J. L., G. Mille, F. Blanc, and J. C. Bertrand (1986), Nitrate reduction activity in a continuous flow-through system in marine-sediments, *Microb. Ecol.*, *12*(3), 283–290.

Estrella, M. R., M. L. Brusseau, R. S. Maier, I. L. Pepper, P. J. Wierenga, and R. M. Miller (1993), Biodegradation, sorption, and transport of 2,4-dichlorophenoxyacetic acid in saturated and unsaturated soils, *Appl. Environ. Microbiol.*, *59*(12), 4266–4273.

Galavotti, H. (2004), Spatial profiles of sediment denitrification at the ground water - surface water interface in Cobb Mill Creek on the Eastern Shore of Virginia, M.S. thesis, Univ. of Va., Charlottesville.

Gu, C. (2007), Hydrological control on nitrate delivery through the groundwater surface water interface, Ph.D. thesis, 250 pp, Univ. of Va., Charlottesville.

Harvey, J. W., and C. C. Fuller (1998), Effect of enhanced manganese oxidation in the hyporheic zone on basin-scale geochemical mass balance, *Water Resour. Res.*, *34*(4), 623–636.

Haycock, N. E., and T. P. Burt (1993), Role of floodplain sediments in reducting the nitrate concentration of subsurface run-off—A case-study in the Cotswold, *UK, Hydrol. Processes*, *7*, 287–295.

Hedin, L. O., J. C. von Fischer, N. E. Ostrom, B. P. Kennedy, M. G. Brown, and G. P. Robertson (1998), Thermodynamic constraints on nitrogen transformations and other biogeochemical processes at soil-stream interfaces, *Ecology*, *79*(2), 684–703.

Hill, A. R. (1996), Nitrate removal in stream riparian zones, *J. Environ. Qual.*, *25*(4), 743–755.

Hill, A. R., K. J. Devito, S. Campagnolo, and K. Sanmugadas (2000), Subsurface denitrification in a forest riparian zone: Interactions between hydrology and supplies of nitrate and organic carbon, *Biogeochemistry*, *51*(2), 193–223.

Hornberger, G. M., and R. C. Spear (1981), An approach to the preliminary-analysis of environmental systems, *J. Environ. Manage.*, *12*(1), 7–18.

Hornberger, G. M., and P. L. Wiberg (2005), *Numerical Methods in Hydrological Science* [e-book], 233 pp., AGU, Washington, D. C.

Hornberger, G. M., K. J. Beven, B. J. Cosby, and D. E. Sappington (1985), Shenandoah Watershed Study - calibration of a topography-based, variable contributing area hydrological model to a small forested catchment, *Water Resour. Res.*, *21*(12), 1841–1850.

Hornberger, G. M., B. J. Cosby, and J. N. Galloway (1986), Modeling the effects of acid deposition: Uncertainty and spatial variability in estimation of long-term sulfate dynamics in a region, *Water Resour. Res.*, *22*(8), 1293–1302.

Jardine, P. M., E. M. Dunnivant, H. M. Selim, and J. F. McCarthy (1992), Comparison of models for describing the transport of dissolved organic-carbon in aquifer columns, *Soil Sci. Soc. Am. J.*, *56*(2), 393–401.

Jones, J. B., and P. J. Mulholland (Eds.) (2000), *Streams and Ground Water*, 425 pp., Academic, San Diego, Calif.

Kelsey, J. W., and M. Alexander (1995), Effect of flow-rate and path-length on P-nitrophenol biodegradation during transport in soil, *Soil Sci. Soc. Am. J.*, *59*(1), 113–117.

Kindred, J. S., and M. A. Celia (1989), Contaminant transport and biodegradation: 2. Conceptual-model and test simulations, *Water Resour. Res.*, *25*(6), 1149–1159.

Kinzelbach, W., W. Schäfer, and J. Herzer (1991), Numerical modeling of natural and enhanced denitrification processes in aquifers, *Water Resour. Res.*, *27*(6), 1123–1135.

Lowrance, R., et al. (1997), Water quality functions of riparian forest buffers in Chesapeake Bay watersheds, *Environ. Manage.*, *21*(5), 687–712.

Maag, M., M. Malinovsky, and S. M. Nielsen (1997), Kinetics and temperature dependence of potential denitrification in riparian soils, *J. Environ. Qual.*, *26*(1), 215–223.

MacQuarrie, K. T. B., E. A. Sudicky, and E. O. Frind (1990), Simulation of biodegradable organic contaminants in groundwater 1. Numerical formulation in principal directions, *Water Resour. Res.*, *26*(2), 207–222.

McKay, M. D., R. J. Beckman, and W. J. Conovert (1979), A comparison of the three methods for selecting values of input variables in the analysis of output from a computer code, *Technometrics*, *21*, 239–245.

Messer, J. J., and P. L. Brezonik (1984), Laboratory evaluation of kinetic-parameters for lake sediment denitrification models, *Ecol. Model.*, *21*(4), 277–286.

Molz, F. J., M. A. Widdowson, and L. D. Benefield (1986), Simulation of microbial-growth dynamics coupled to nutrient and oxygen-transport in porous media, *Water Resour. Res.*, *22*(8), 1207–1216.

Murray, R. E., L. L. Parsons, and M. S. Smith (1989), Kinetics of nitrate utilization by mixed populations of denitrifying bacteria, *Appl. Environ. Microbiol.*, *55*(3), 717–721.

Ocampo, C. J., C. E. Oldham, and M. Sivapalan (2006), Nitrate attenuation in agricultural catchments: Shifting balances between transport and reaction, *Water Resour. Res.*, *42*, W01408, doi:10.1029/2004WR003773.

Oremland, R. S., C. Umberger, C. W. Culbertson, and R. L. Smith (1984), Denitrification in San-Francisco Bay intertidal sediments, *Appl. Environ. Microbiol.*, *47*(5), 1106–1112.

Parlange, J. Y., J. L. Starr, D. A. Barry, and R. D. Braddock (1984), Some approximate solutions of the transport-equation with irreversible reactions, *Soil Sci.*, *137*(6), 434–442.

Phillips, P. J., J. M. Denver, R. J. Shedlock, and P. A. Hamilton (1993), Effect of forested wetlands on nitrate concentrations in ground-water and surface-water on the Delmarva Peninsula, *Wetlands*, *13*(2), 75–83.

Puckett, L. J., and W. B. Hughes (2005), Transport and fate of nitrate and pesticides: Hydrogeology and riparian zone processes, *J. Environ. Qual.*, *34*(6), 2278–2292.

Robertson, W. D., and J. A. Cherry (1995), In-situ denitrification of septic-system nitrate using reactive porous-media barriers—Field trials, *Ground Water*, *33*(1), 99–111.

Runkel, R. L., and S. C. Chapra (1993), An efficient numerical-solution of the transient storage equations for solute transport in small streams, *Water Resour. Res.*, *29*(1), 211–215.

Schiff, S. L., K. J. Devito, R. J. Elgood, P. M. McCrindle, J. Spoelstra, and P. Dillon (2002), Two adjacent forested catchments: Dramatically different NO_3^- export, *Water Resour. Res.*, *38*(12), 1292, doi:10.1029/2000WR000170.

Schipper, L. A., A. B. Cooper, C. G. Harfoot, and W. J. Dyck (1993), Regulators of denitrification in an organic riparian soil, *Soil Biol. Biochem.*, *25*(7), 925–933.

Sheibley, R. W., J. H. Duff, A. P. Jackman, and F. J. Triska (2003a), Inorganic nitrogen transformations in the bed of the Shingobee River, Minnesota: integrating hydrologic and biological processes using sediment perfusion cores, *Limnol. Oceanogr.*, *48*(3), 1129–1140.

Sheibley, R. W., A. P. Jackman, J. H. Duff, and F. J. Triska (2003b), Numerical modeling of coupled nitrification-denitrification in sediment perfusion cores from the hyporheic zone of the Shingobee River, MN, *Adv. Water Res.*, *26*(9), 977–987.

Starr, J. L., F. Broadbent, and D. R. Nielsen (1974), Nitrogen transformations during continuous leaching, *Soil Sci. Soc. Am. Proc.*, *38*(2), 283–289.

Toride, N., et al. (1995), The CXTFIT code for estimating transport parameters from laboratory or field tracer experiments, version 2.0, research report, U.S. Salinity Lab., Agric. Res. Serv., U.S. Dep. of Agric., Riverside, Calif.

Vidon, P. G. F., and A. R. Hill (2004), Landscape controls on the hydrology of stream riparian zones, *J. Hydrol.*, *292*(1–4), 210–228.

Weiskel, P. K., and B. L. Howes (1991), Quantifying dissolved nitrogen flux through a coastal watershed, *Water Resour. Res.*, *27*(11), 2929–2939.

Whitmire, S. L., and S. K. Hamilton (2005), Rapid removal of nitrate and sulfate in freshwater wetland sediments, *J. Environ. Qual.*, *34*(6), 2062–2071.

Widdowson, M. A., F. J. Molz, and L. D. Benefield (1988), A numerical transport model for oxygen- and nitrate-based respiration linked to substrate and nutrient availability in porous media, *Water Resour. Res.*, *24*(9), 1553–1565.

S. A. Flewelling, J. S. Herman, G. M. Hornberger, and A. L. Mills, Department of Environmental Sciences, University of Virginia, Charlottesville, VA 22904-4123, USA. (saf5f@virginia.edu; jherman@virginia.edu; gmh3k@virginia.edu; amills@virginia.edu)

C. Gu, Berkeley Water Center, University of California, Berkeley, CA 94729, USA. (cgu@berkeley.edu)